Article

Cell Reports

Glutamate Receptor Modulation Is Restricted to Synaptic Microdomains

Graphical Abstract

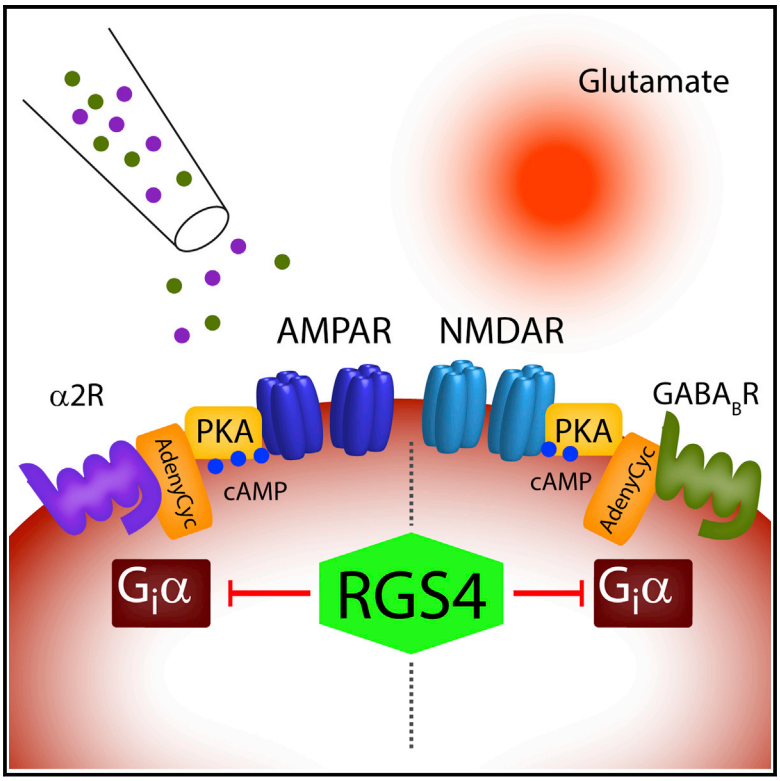

Authors

Gyorgy Lur, Michael J. Higley

Correspondence

m.higley@yale.edu

In Brief

Lur and Higley demonstrate that norepinephrine and GABA differentially regulate AMPAR-mediated currents and NMDAR-mediated Ca^{2+} influx, respectively. These distinct actions are driven by downregulation of PKA signaling and occur due to the existence of functional microdomains that are maintained by receptor co-localization and the actions of RGS4.

Highlights

- Adrenergic α2Rs reduce AMPAR currents while $GABA_BRs$ reduce NMDAR Ca^{2+} influx
- Adrenergic and GABAergic control of glutamate receptors occurs via inhibition of PKA
- Modulatory microdomains are established by co-localization and the actions of RGS4

Lur & Higley, 2015, Cell Reports *12*, 326–334
July 14, 2015
http://dx.doi.org/10.1016/j.celrep.2015.06.029

CellPress

OPEN ACCESS
CellPress

Cell Reports
Article

Glutamate Receptor Modulation Is Restricted to Synaptic Microdomains

Gyorgy Lur[1] and Michael J. Higley[1,*]
[1]Department of Neurobiology, Program in Cellular Neuroscience, Neurodegeneration and Repair, Yale School of Medicine, New Haven, CT 06510, USA
*Correspondence: m.higley@yale.edu
http://dx.doi.org/10.1016/j.celrep.2015.06.029

SUMMARY

A diverse array of neuromodulators governs cellular function in the prefrontal cortex (PFC) via the activation of G-protein-coupled receptors (GPCRs). However, these functionally diverse signals are carried and amplified by a relatively small assortment of intracellular second messengers. Here, we examine whether two distinct $G\alpha_i$-coupled neuromodulators (norepinephrine and GABA) act as redundant regulators of glutamatergic synaptic transmission. Our results reveal that, within single dendritic spines of layer 5 pyramidal neurons, alpha-2 adrenergic receptors (α2Rs) selectively inhibit excitatory transmission mediated by AMPA-type glutamate receptors, while type B GABA receptors ($GABA_BRs$) inhibit NMDA-type receptors. We show that both modulators act via the downregulation of cAMP and PKA. However, by restricting the lifetime of active $G\alpha_i$, RGS4 promotes the independent control of these two distinct target proteins. Our findings highlight a mechanism by which neuromodulatory microdomains can be established in subcellular compartments such as dendritic spines.

INTRODUCTION

Neuromodulation via G protein-coupled receptors (GPCRs) provides a ubiquitous mechanism for regulating neuronal activity in the mammalian brain. In contrast to classical neurotransmitters that directly excite or inhibit postsynaptic neurons, neuromodulators alter neuronal excitability and modify synaptic transmission (Destexhe et al., 1994; Dismukes, 1979). Interestingly, there is a paradoxical mismatch between the diversity of modulatory ligands and the relative paucity of GPCR-linked second messenger systems such as adenylate cyclase and phospholipase C. The mobility of dissociated G protein subunits and downstream molecules such as calcium (Ca^{2+}), cAMP, and inositol-1,4,5-triphosphate should further reduce the cellular capacity for segregated signaling pathways. Nevertheless, there is evidence for the functional compartmentalization of soluble messengers into independent microdomains, which could contribute to neuromodulatory specificity. For example, rapid intracellular buffering coupled with potent extrusion mechanisms spatially restricts Ca^{2+} within presynaptic terminals and dendritic spines (Higley and Sabatini, 2008; Lisman et al., 2007; Yuste et al., 2000). However, the potential for mobile, non-ionic signaling molecules to be isolated within synaptic microdomains is largely unknown.

In the prefrontal cortex (PFC), neuromodulation by both norepinephrine (NE) and gamma-amino butyric acid (GABA) regulates higher cognitive functions, including attention and short-term "working" memory (Gamo and Arnsten, 2011; Kesner and Churchwell, 2011). Altered levels of NE and GABA are also linked to neuropsychiatric disorders, such as schizophrenia, attention deficit, and addiction (Arnsten, 2011; Stan and Lewis, 2012; Tyacke et al., 2010). Experimental evidence suggests that both type 2 alpha adrenergic receptors (α2Rs) and type B GABA receptors ($GABA_BRs$) modulate excitatory glutamatergic signaling in the PFC (Chalifoux and Carter, 2010; Ji et al., 2008; Liu et al., 2006). Additionally, ultrastructural studies have localized both α2Rs and $GABA_BRs$ to dendritic spines, the location of synaptic glutamate receptors (Kulik et al., 2003; Wang et al., 2007). Both α2Rs and $GABA_BRs$ are GPCRs coupled to the G protein subunit $G\alpha_i$, whose activation leads to the inhibition of adenylate cyclase and decreased production of cAMP (Knight and Bowery, 1996; Summers and McMartin, 1993). The subsequent reduction in cAMP-dependent protein kinase (PKA) activity provides a potential mechanism for the control of both AMPA- and NMDA-type glutamate receptors (AMPARs and NMDARs, respectively) (Chen et al., 2008; Esteban et al., 2003; Raymond et al., 1994). These observations raise the question of whether α2Rs and $GABA_BRs$ act as redundant modulators of prefrontal synaptic transmission.

To test this hypothesis, we combined electrophysiological recordings and two-photon imaging of PFC pyramidal neurons with optical stimulation of excitatory glutamatergic synapses using focal glutamate uncaging (Carter and Sabatini, 2004). Our results reveal the surprising observation that activating α2Rs reduces AMPAR-mediated responses, whereas activating $GABA_BRs$ decreases NMDAR-mediated responses. Notably, both modulatory pathways utilize $G\alpha_i$-mediated downregulation of cAMP and PKA signaling, and this dissociation occurs despite functional evidence that both α2Rs and $GABA_BRs$ are located in the same dendritic spines. We further find that inhibiting the GTPase activating protein RGS4 eliminates the selective compartmentalization of adrenergic and GABAergic actions. Thus, RGS4 promotes the independent control of two distinct

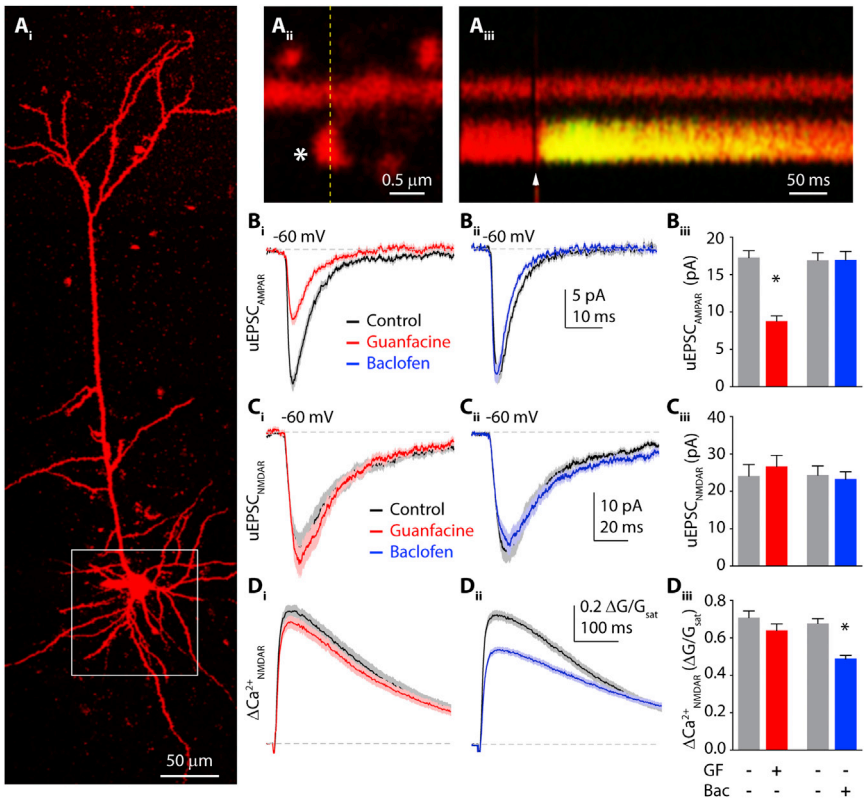

Figure 1. α2Rs and $GABA_BRs$ Differentially Modulate AMPA- and NMDA-type Glutamate Receptors

(A) (i) Two-photon image of a layer 5 pyramidal neuron filled with Alexa Fluor 594 dye via the patch pipette. White box indicates the basal dendritic arbor. (ii) Close-up image of a dendritic spine. Asterisk shows the location of glutamate uncaging. (iii) Fluorescence collected in a line scan indicated on (ii) by dashed line. Arrowhead shows the time point of glutamate uncaging.

(B) (i) Mean AMPAR-mediated uEPSCs in control (black) and guanfacine (red) ±SEM (shaded areas). (ii) AMPAR-mediated uEPSCs in control (black) and baclofen (blue) ±SEM (shaded areas). (iii) Bars represent mean uEPSC amplitudes in control (gray), guanfacine (red), and baclofen (blue) ±SEM.

(C and D) (Ci) 2PLU-evoked NMDAR-currents and (Di) Ca^{2+} transients in control (black) and guanfacine (red), mean (solid lines) ±SEM (shaded areas). (Cii) NMDAR-mediated uEPSCs and (Dii) Ca^{2+} transients in control (black) and baclofen (blue) ±SEM (shaded areas). (Ciii) Bars represent mean uEPSC amplitudes in control (gray), guanfacine (red), and baclofen (blue) ±SEM (Diii).

Mean amplitude of NMDAR Ca^{2+} transients in control (gray), guanfacine (red), and baclofen (blue) ±SEM. *p < 0.05, unpaired t test.

target proteins by eliminating crosstalk between signaling pathways in dendritic spines. Our results highlight a novel mechanism by which biochemical multiplexing can occur in subcellular microdomains.

RESULTS

Distinct $G\alpha_i$-Coupled Agonists Differentially Modulate Postsynaptic Glutamate Receptors

We investigated whether two distinct neuromodulators that target the same biochemical pathway produce similar changes in glutamatergic transmission. To identify the actions of α2Rs and $GABA_BRs$ on postsynaptic glutamatergic signaling, we used two-photon laser uncaging of glutamate (2PLU) to stimulate single excitatory synapses on prefrontal L5 pyramidal neurons while recording excitatory postsynaptic currents (uEPSCs) and imaging postsynaptic calcium (Ca^{2+}) signals. Uncaging power was individually calibrated for spines on the proximal basal dendrites (<100 μm from the soma) to emulate endogenous glutamate release from a single presynaptic terminal (Figures 1A and S1).

First, we pharmacologically isolated AMPAR-mediated responses and recorded synaptic currents (Figure 1B; see Experimental Procedures). Bath application of the α2R agonist guanfacine (40 μM) reduced uEPSCs from 17.2 ± 0.9 pA (n = 32 spines) to 8.8 ± 0.7 pA (n = 32 spines, p < 0.0001, unpaired t test). In contrast, the $GABA_BR$ agonist baclofen (5 μM) had no effect on AMPAR-mediated uEPSC amplitude (16.9 ± 1.0 pA, n = 26 spines versus 16.9 ± 1.1 pA, n = 30 spines, p = 0.97). We then performed converse experiments in which we isolated NMDAR-mediated responses and recorded both uEPSCs and ΔCa^{2+} in the spine head (Figures 1C and 1D; see Supplemental Experimental Procedures). Under these conditions, 2PLU-evoked ΔCa^{2+} is mediated by influx through NMDARs (Figure S2). Guanfacine had no effect on either uEPSC amplitude (24.1 ± 3.1 pA, n = 38 spines, versus 26.6 ± 2.9 pA, n = 32 spines, p = 0.56) or ΔCa^{2+} (0.71 ± 0.035 $\Delta G/G_{sat}$ versus 0.64 ± 0.034 $\Delta G/G_{sat}$, p = 0.17). In contrast, baclofen significantly reduced NMDAR-mediated ΔCa^{2+} in the spine head (0.68 ± 0.03 $\Delta G/G_{sat}$, n = 33 spines versus 0.49 ± 0.02 $\Delta G/G_{sat}$, n = 35 spines, p < 0.0001) but did not alter uEPSCs (24.3 ± 2.5 pA, versus 23.2 ± 2.0 pA, p = 0.73). Thus, our results demonstrate that α2Rs and $GABA_BRs$ selectively modulate postsynaptic AMPARs and NMDARs, respectively.

Modulation of AMPARs and NMDARs Is Mediated by Downregulation of PKA

One explanation for our results is that adrenergic and GABAergic modulation of glutamate receptors occurs via distinct biochemical signaling pathways. We therefore isolated AMPAR-mediated synaptic responses and tested the ability of H89 (10 μM), a selective blocker of cAMP-dependent kinase (PKA), to mimic and occlude the actions of guanfacine. In the presence of H89, uEPSC amplitude was 12.4 ± 1.3 pA (n = 30 spines, Figures 2A and 2B). In the combined presence of H89 and guanfacine, uEPSC amplitude was 9.0 ± 0.6 pA (n = 35 spines, Figures 2A

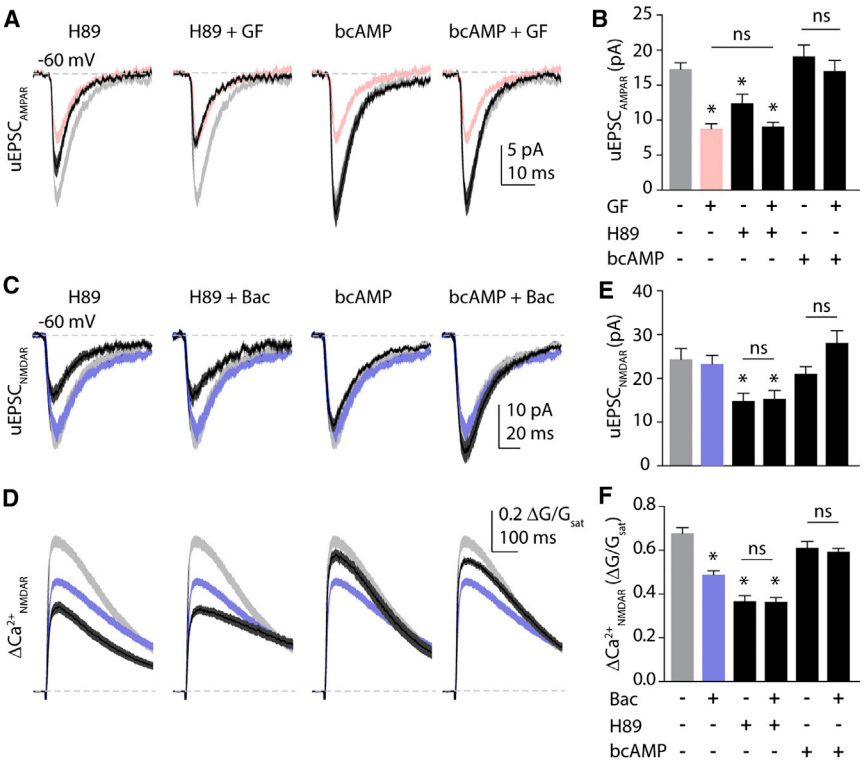

Figure 2. Both α2R Modulation of AMPARs and $GABA_BR$ Modulation of NMDARs Are Mediated by Downregulation of PKA

(A) AMPAR-mediated uEPSCs. Solid black lines show mean ± SEM (dark gray shading) for responses in the PKA antagonist H89 (10 μM), H89 + guanfacine (40 μM), the PKA activator N-6-benzo-cAMP (bcAMP, 100 μM), or bcAMP + guanfacine (left to right). Light gray and red shaded areas represent mean ± SEM of control and guanfacine groups, respectively, for comparison.

(B) Bars represent mean amplitudes ±SEM of uEPSC under the above conditions.

(C) NMDAR-mediated uEPSCs. Solid black lines show mean ± SEM (dark gray shading) for responses in the PKA antagonist H89 (10 μM), H89 + baclofen (5 μM), the PKA activator bcAMP (100 μM), or bcAMP + baclofen (left to right). Light gray and blue shaded areas represent mean ± SEM of control and baclofen groups, respectively, for comparison.

(D) 2PLU-evoked Ca^{2+} transients under the same conditions as in (C).

(E and F) Bars represent mean amplitudes ±SEM of uEPSC (E) and Ca^{2+} transients under the above conditions (F).

*$p < 0.05$, Tukey's multiple comparison test.

and 2B). We also examined the actions of the selective PKA activator and cAMP analog N6-benzo-cAMP (bcAMP, 100 μM). In the presence of bcAMP, uEPSC amplitude was 19.1 ± 1.7 pA (n = 30 spines). Combined application of bcAMP and guanfacine produced a uEPSC amplitude of 17.0 ± 1.5 pA (n = 31 spines). A one-way ANOVA comparing all groups revealed significant differences ($F = 19.57$, $p < 0.0001$) that we explored using post hoc comparisons (significant for $p < 0.05$, Tukey's test). These analyses revealed that H89 both mimicked and occluded the actions of guanfacine, whereas bcAMP blocked the actions of guanfacine (Figures 2A and 2B).

In a parallel set of studies, we isolated NMDARs and examined the biochemical mechanisms underlying their modulation by baclofen. In the presence of H89, the NMDAR-mediated uEPSC was 14.8 ± 1.8 pA (n = 29 spines) and the ΔCa^{2+} was 0.37 ± 0.03 $\Delta G/G_{sat}$. Co-application of H89 and baclofen yielded a uEPSC of 15.3 ± 1.9 pA (n = 29 spines) and a ΔCa^{2+} of 0.36 ± 0.02 $\Delta G/G_{sat}$. After bcAMP, the uEPSC was 21.0 ± 1.6 pA and ΔCa^{2+} was 0.61 ± 0.03 $\Delta G/G_{sat}$ (n = 30 spines), while combined bcAMP and baclofen produced a uEPSC of 28.0 ± 2.8 pA and a ΔCa^{2+} of 0.59 ± 0.02 $\Delta G/G_{sat}$ (n = 31 spines, Figures 2C–2F). As above, Tukey's post hoc tests (ANOVA, $F = 43.48$, $p < 0.0001$) revealed that H89 occluded and bcAMP blocked the actions of baclofen on NMDAR-mediated responses (Figures 2C–2F).

Our data indicate that both α2Rs and $GABA_BRs$ exert control of glutamate receptors via a downregulation of PKA signaling. Phosphorylation of the Serine 845 (S845) residue of the GluA1 subunit is known to regulate AMPA-receptor stability and membrane trafficking (Esteban et al., 2003). We therefore probed whether guanfacine or baclofen altered S845 phosphorylation. Assays were performed on four to six independent samples, and one-way ANOVA revealed significant effects ($F = 19.81$, $p < 0.0001$) that were investigated with post hoc analyses (Figures 3A and 3B). In comparison to untreated PFC tissue, 10-min incubation with either guanfacine or H89 significantly reduced S845 phosphorylation, while baclofen had no effect. In addition, the adenylate cyclase activator forskolin (50 μM) significantly increased the phosphorylation of AMPARs relative to control.

A recent study identified a novel PKA phosphorylation site on the GluN2B subunit, Serine 1166 (S1166), which modulates the Ca^{2+} permeability of NMDARs (Murphy et al., 2014). In keeping with our Ca^{2+} imaging data, we found that application of either baclofen or H89, but not guanfacine, reduced S1166 phosphorylation. Conversely, forskolin enhanced the phosphorylation of the same residue (Figures 3C and 3D, one-way ANOVA, $F = 20.48$, $p < 0.0001$, Tukey's post hoc test). These results suggest the involvement of S1166 in the GABAergic regulation of Ca^{2+} influx through NMDARs, though we cannot rule out the participation of other PKA targets.

To confirm that functional GluN2B subunits contribute to 2PLU-evoked NMDAR responses in our recordings, we measured NMDAR activation in the presence of the specific GluN2B antagonist ifenprodil (3 μM). Ifenprodil significantly reduced NMDAR currents (22.7 ± 1.8 pA, n = 46 spines versus 14.0 ± 1.4 pA, n = 33 spines, $p = 0.0006$, Figures S2C and S2D) and ΔCa^{2+} (0.54 ± 0.02 $\Delta G/G_{sat}$, n = 46 spines versus 0.44 ± 0.02 $\Delta G/G_{sat}$, n = 33 spines, $p = 0.0003$, Figure S2). Thus, baclofen but not guanfacine diminishes synaptic Ca^{2+} influx through NMDARs via the dephosphorylation of the GluN2B

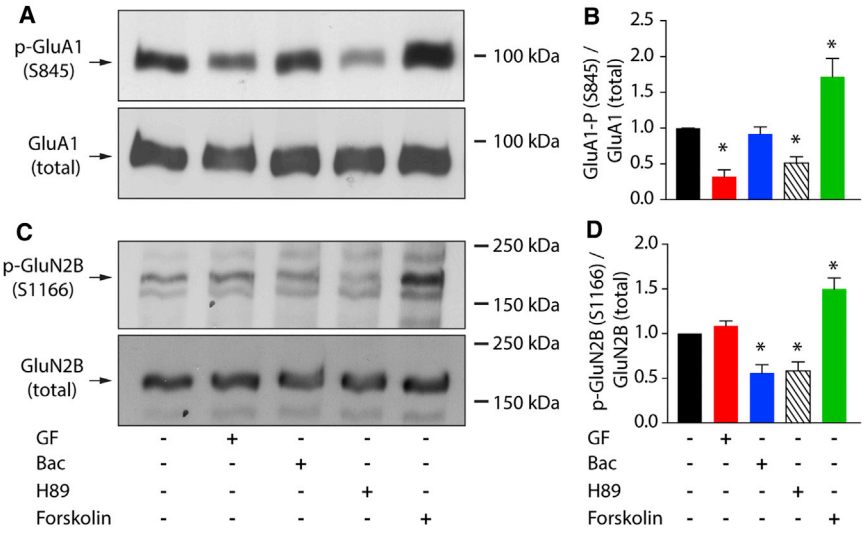

Figure 3. α2R and $GABA_BR$ Activation Reduces GluA1 (S845) and GluN2B (S1166) Phosphorylation in the PFC, Respectively

(A) Western blot for phosphorylated GluA1 (S845) in prefrontal tissue lysates, left to right: under control (n = 6 animals), guanfacine (40 μM, n = 5 animals), baclofen (5 μM, n = 5 animals), H89 (10 μM, n = 5 animals), or forskolin (50 μM, n = 4 animals) conditions (top). Membranes were then re-blotted for total GluA1 (bottom).

(B) Quantification of S845 phosphorylation. Bars show mean ± SEM normalized to control (black) in guanfacine (red), baclofen (blue), H89 (striped), and forskolin (green).

(C) Western blots depicting GluN2B (S1166) phosphorylation (top) and total GluN2B (bottom) in, left to right: control (n = 5 animals), guanfacine (40 μM, n = 6 animals), baclofen (5 μM, n = 6 animals), H89 (10 μM, n = 5 animals), or forskolin (50 μM, n = 5 animals).

(D) Bars represent mean ± SEM. S1166 phosphorylation in control (black), guanfacine (red), baclofen (blue), H89 (striped), and forskolin (green).

*p < 0.05, Tukey's multiple comparison test.

subunit at the Serine 1166 residue. In summary, these results confirm that the surprisingly disparate actions of α2Rs and $GABA_BRs$ on glutamate receptors are all mediated by downregulation of PKA signaling.

Adrenergic and GABAergic Actions Are Localized to the Same Dendritic Spine

As our initial studies compared separate populations of spines in control and treatment conditions, one explanation for our findings is that either guanfacine or baclofen may act non-cell-autonomously such that the two PKA-dependent signaling pathways occur in different cells. To test this possibility, we co-applied guanfacine and baclofen while stimulating a single synapse using 2PLU. We monitored both uEPSCs and ΔCa^{2+} while voltage clamping the cell at either −70 mV or +40 mV to measure AMPAR- or NMDAR-mediated responses, respectively (Figure 4). Compared to baseline, combined application of guanfacine and baclofen for 10 min decreased AMPAR currents (18.8 ± 2.8 pA versus 12.1 ± 1.7 pA, n = 6 spines, p = 0.0163, paired t test, Figure 4A). As above, the drug combination did not change NMDAR-mediated currents (12.7 ± 2.5 pA versus 15.6 ± 5.1 pA, n = 6 spines, p = 0.9220, paired t test, Figure 4B) but decreased ΔCa^{2+} (0.21 ± 0.04 $\Delta G/G_{sat}$ versus 0.12 ± 0.03 $\Delta G/G_{sat}$, p = 0.0132, paired t tests, Figure 4C). Importantly, the combined actions of guanfacine and baclofen on AMPAR-mediated currents (n = 6 spines, p = 0.626, paired t test) and NMDAR-mediated Ca^{2+} influx (n = 6 spines, p = 0.6555, paired t test) were occluded by adding the membrane-impermeable PKA antagonist PKI(6-22) (20 μM) to the recording pipette (Figures 4A–4C). These results confirm that the PKA-dependent actions of α2Rs and $GABA_BRs$ cell-autonomously modulate both types of glutamate receptors.

Our results might also be explained if α2Rs and $GABA_BRs$ are not co-localized, giving rise to a physical segregation of signaling pathways that could produce a functional dissociation. To test this possibility, we performed three sets of experiments. First, we used a puffer pipette to locally apply a combination of guanfacine and baclofen to a small dendritic region while holding the cell at either −70 mV or +40 mV (Figures 5A–5D). This focal drug application yielded similar results to bath application. AMPAR-mediated currents were decreased (19.7 ± 2.6 pA to 9.3 ± 1.9 pA, n = 10, p = 0.0083), NMDAR-mediated currents were not altered (11.4 ± 2.1 pA versus 10.7 ± 2.1 pA, n = 10, p = 0.39), and NMDAR-mediated ΔCa^{2+} was decreased (0.22 ± 0.05 $\Delta G/G_{sat}$ versus 0.088 ± 0.02 $\Delta G/G_{sat,}$ n = 10, p = 0.0055).

Second, we performed immunohistochemical triple-staining to test for co-localization of α2Rs and $GABA_BRs$ at the postsynaptic density (Figures 5E and 5F; see Supplemental Experimental Procedures). α2Rs and $GABA_BRs$ were significantly more co-localized with the postsynaptic protein PSD95 than the presynaptic marker bassoon or a pixel-shuffled control.

Third, we tested the actions of α2Rs and $GABA_BRs$ on voltage-gated calcium channels (VGCCs), known to be modulated by a PKA-independent pathway involving the membrane delimited beta-gamma subunits ($G\beta\gamma$) associated with $G\alpha_i$ (Herlitze et al., 1996; Yan and Surmeier, 1996). We monitored VGCC-dependent ΔCa^{2+} in spines and adjacent dendritic shafts evoked by back-propagating action potentials (bAPs, Figure S3; see Experimental Procedures) (Sabatini and Svoboda, 2000). Under control conditions, ΔCa^{2+} in spines was 0.052 ± 0.003 $\Delta G/G_{sat}$ (n = 34 spines). In the presence of either guanfacine or baclofen, ΔCa^{2+} was 0.029 ± 0.002 $\Delta G/G_{sat}$ (n = 38 spines) or 0.031 ± 0.001 $\Delta G/G_{sat}$ (n = 41 spines), respectively. Combined application of guanfacine and baclofen produced a ΔCa^{2+} of 0.036 ± 0.003 $\Delta G/G_{sat}$ (n = 33 spines, Figures S3B–S3E). One-way ANOVA (F = 20.52, p < 0.0001) with post hoc testing revealed that both guanfacine and baclofen significantly reduced ΔCa^{2+}, but there was no additional effect of combining the two drugs. Similar results were seen for ΔCa^{2+} in the corresponding dendritic shafts. These results indicate modulation of physically overlapping pools of VGCCs. Thus, the combination of findings

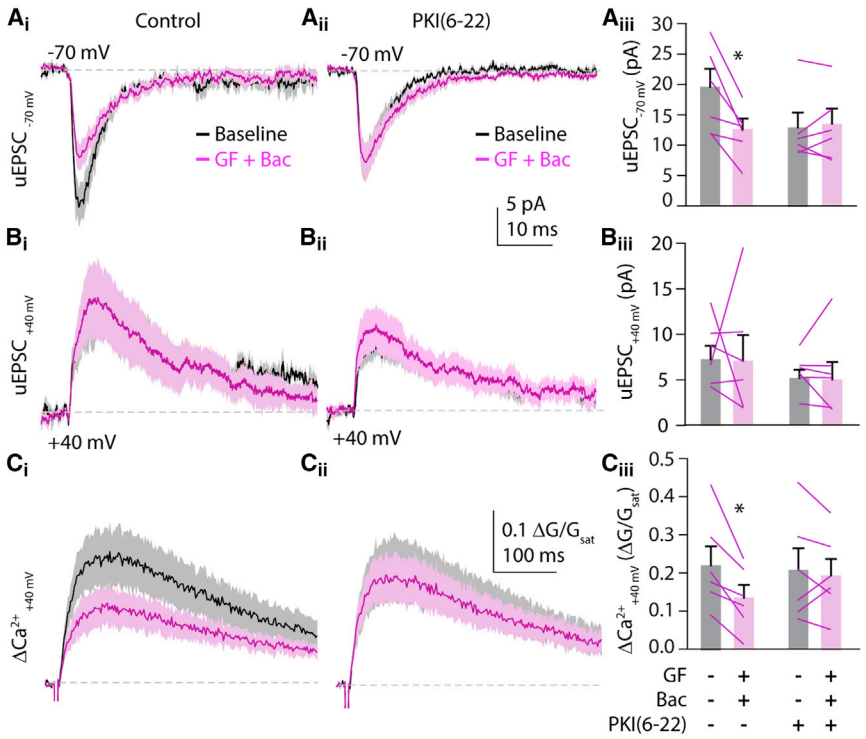

Figure 4. α2Rs and $GABA_BRs$ Cell Autonomously Modulate Glutamate Receptors

(Ai and Bi) (Ai) Mean ± SEM traces (solid lines and shaded areas, respectively) of 2PLU-evoked uEPSCs from a single spine with the cell voltage clamped at −70 mV or at (Bi) +40 mV to measure AMPAR- and NMDAR-mediated currents, respectively. Black traces are uEPSCs during baseline recording, magenta traces show currents following 10 min exposure to guanfacine plus baclofen (n = 6 spines on six cells).

(Ci) Mean ± SEM traces (solid lines and shaded areas, respectively) showing ΔCa^{2+} traces with the cell voltage clamped at +40 mV during baseline (black) and after guanfacine plus baclofen flow in (magenta).

(Aii–Cii) Same experiment as in (Ai)–(Ci), but with the membrane-impermeable PKA inhibitor PKI(6-22) (20 μM) in the recording pipette (n = 6 spines on six cells).

(Aiii and Biii) Mean ± SEM uEPSC amplitudes (bars) and for each individual cell (lines) recorded at −70 or +40 mV holding potential during baseline (gray) and post guanfacine and baclofen (magenta) using control- or PKI(6-22)-containing pipette solution.

(Ciii) As above for NMDAR-mediated Ca^{2+} transients.

*$p < 0.05$, paired t test.

strongly supports the conclusion that α2Rs and $GABA_BRs$ are co-localized in the same dendritic spines.

Preferential Structural Co-localization of GPCRs with Glutamate Receptors

Our results indicate functional coupling of α2Rs with AMPARs and $GABA_BRs$ with NMDARs. To determine whether these receptor groupings have a structural underpinning, we performed a proximity ligation assay that identifies proteins localized within 10–15 nm from each other (Söderberg et al., 2006). Co-staining for GluA1 and α2R produced significantly higher labeling density than for GluA1 and $GABA_BR$ (1.7 ± 0.2 versus 0.9 ± 0.1 puncta per 100 μm^2, n = 31 images from three mice, p = 0.0004). Similarly, co-staining for NR1 and $GABA_BR$ produced significantly higher labeling density than for NR1 and α2R (1.2 ± 0.09 versus 0.76 ± 0.08 puncta per 100 μm^2, n = 31 images from three mice, p = 0.0004, Figure 6). This preferential structural localization of α2Rs/AMPARs and $GABA_BRs$/NMDARs at synapses suggests the existence of synaptic microdomains where neuromodulation can occur independently despite utilization of similar biochemical signaling pathways.

RGS4 Limits the Crosstalk between Different $G\alpha_i$-Coupled Receptors

Our results suggest the surprising conclusion that separate, parallel modulation of glutamate receptors occurs without biochemical crosstalk in single spines. Notably, although activation of $G_{i/o}$-coupled receptors decreases the amount of cAMP and active PKA in the spine, the concentration of the active mobile $G\alpha_i$ subunit is increased. Thus, some mechanism must limit the functional mobility of $G\alpha_i$ to prevent signaling crosstalk. One such mechanism might involve Regulators of G protein Signaling (RGS) proteins that accelerate hydrolysis of GTP to GDP, hastening the self-inactivation of $G\alpha_i$ (Arshavsky and Pugh, 1998; Watson et al., 1996; Zhong et al., 2003). To test this possibility, we measured 2PLU-evoked synaptic currents and corresponding Ca^{2+} transients in the presence of a selective small molecule inhibitor (CCG50014; Blazer et al., 2011; Turner et al., 2012) that targets RGS4, the most abundant RGS family member in layer 5 pyramidal neurons of the PFC (Ebert et al., 2006; Gold et al., 1997).

CCG50014 (5 μM) by itself did not alter responses mediated by either NMDARs or AMPARs (Figures 7A–7C). However, in contrast to our earlier findings, in the presence of CCG50014, baclofen produced a significant reduction in AMPAR-mediated currents (17.5 ± 1.6 pA, n = 31 spines versus 10.0 ± 1.1 pA, n = 32 spines, $p < 0.001$). Guanfacine also reduced AMPAR-mediated currents (to 9.7 ± 0.8 pA, n = 30 spines, $p < 0.001$) similarly to guanfacine alone ($p > 0.05$) (Figure 7A). Conversely, in the presence of CCG50014, guanfacine produced a significant reduction in NMDAR-mediated currents (27.6 ± 2.8 pA, n = 30 spines versus 15.4 ± 2.4, n = 32 spines, $p < 0.01$) and ΔCa^{2+} (0.68 ± 0.03 $\Delta G/G_{sat}$ versus 0.5 ± 0.03 $\Delta G/G_{sat}$, $p < 0.001$, Figures 7B and 7C). Notably, in combination with CCG50014, baclofen also reduced NMDAR-mediated currents (to 7.8 ± 1.2 pA, n = 35 spines, $p < 0.001$; Figures 7A and 7C) and ΔCa^{2+} (to 0.37 ± 0.03 $\Delta G/G_{sat}$ in CCG50014+baclofen, $p < 0.001$; Figures 7B and 7C).

To confirm the specificity of our results, we dialyzed neurons with an antibody against RGS4 via the patch pipette, a method

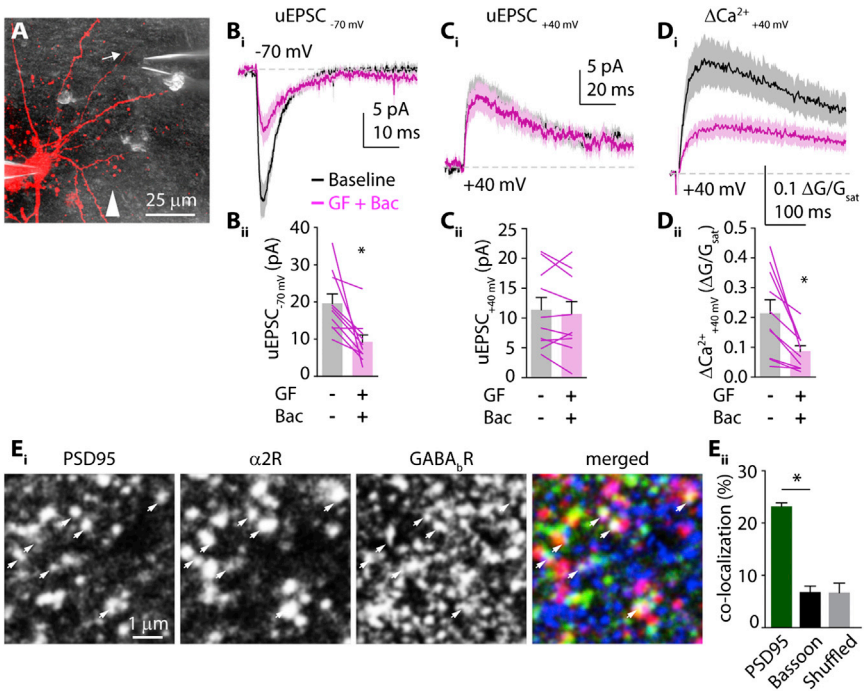

Figure 5. α2Rs and $GABA_BRs$ Are in the Same Dendritic Spine

(A) Two-photon image of a L5 pyramidal neuron (red) and two-photon differential interference contrast (DIC) image (gray) showing the puffer pipette near the recorded denritic spine (arrow). White arrowhead is pointing in the direction of ACSF flow in the chamber.

(Bi–Di) (Bi) Mean ± SEM uEPSC traces (solid lines and shaded areas, respectively) of 2PLU-evoked uEPSCs from a single spine with the cell voltage clamped at −70 mV or at (Ci and Di) +40 mV to measure AMPAR- and NMDAR-mediated currents and Ca^{2+} influx, respectively. Black traces are uEPSCs during baseline recording, magenta traces show currents following 10 min exposure to locally applied guanfacine plus baclofen (n = 10 spines on ten cells).

(Aii–Cii) uEPSC and Ca^{2+} transient amplitudes: mean ± SEM (bars) and for each individual cell separately (lines) recorded at −70 or +40 mV holding potential during baseline (gray) and post-guanfacine and baclofen (magenta).

(Ei) Representative confocal images of PSD95 (green), α2R (red), and $GABA_BR$ (blue) co-staining. White arrows point to both GPCRs co-localizing with PSD95.

(Eii) Bars showing average co-localization of both α2Rs and $GABA_BRs$ with PSD95 (green) or Bassoon (black) in original or pixel-shifted (gray) images.

previously shown to specifically inhibit RGS4 function (Liu et al., 2006), and performed similar experiments (Figure S4). We found that, with the RGS4 antibody in the pipette solution, baclofen significantly reduced AMPAR-mediated currents (21.1 ± 1.6 pA, n = 30 spines versus 14.14 ± 0.98 pA, n = 32 spines, p = 0.0003). In complementary experiments, in the presence of the RGS4 antibody, guanfacine reduced NMDAR-mediated currents (20.7 ± 2 pA, n = 31 spines versus 7.15 ± 1.3 pA, n = 34 spines, $p < 0.0001$) and ΔCa^{2+} (0.633 ± 0.017 $\Delta G/G_{sat}$ versus 0.34 ± 0.02 $\Delta G/G_{sat}$, $p < 0.0001$). In conclusion, our data indicate that RGS4 prevents crosstalk between biochemical signaling cascades and preserves neuromodulatory specificity.

DISCUSSION

Multiple neuromodulatory systems coupled to GPCRs share common signal transduction pathways. In the prefrontal cortex, neuronal activity is regulated by $G\alpha_i$-mediated signaling through receptors for norepinephrine, GABA, dopamine (D2), and acetylcholine (M2, M4). However, it remains largely unknown how individual neurons distinguish between these modulatory inputs and prevent crosstalk between similar biochemical signaling pathways. Here, we found that activation of α2Rs and $GABA_BRs$ selectively inhibits AMPARs and NMDARs, respectively, and that this modulation occurs at single glutamatergic synapses. In both cases, the regulation of glutamate receptors occurs via a $G\alpha_i$-dependent reduction in PKA activity. Our evidence suggests that all four receptors are present in individual spines with a preferential co-localization (<20 nm) of α2Rs/AMPARs and $GABA_BRs$/NMDARs. Under control conditions, crosstalk between α2R- and $GABA_BR$-coupled signaling cascades is prevented by the actions of RGS4, a GTPase Activating Protein (GAP) that targets $G\alpha_i$ (Watson et al., 1996). Our results provide evidence for a novel mechanism by which biochemical signaling pathways are functionally compartmentalized and highlight the role of RGS4 in regulating synaptic transmission (Figure S5). In future studies, it will be interesting to determine whether other modulatory pathways (e.g., D2 dopamine receptors) obey similar compartmentalization to regulate specific glutamate receptors.

Establishment of Synaptic Microdomains for Neuromodulation

Our data show that, under control conditions, there is no crosstalk between α2R- and $GABA_BR$-mediated modulation of glutamate receptors despite similar actions on cAMP and PKA activity. One explanation for this compartmentalization is that α2Rs and $GABA_BRs$ are located on different dendritic spines. We excluded this possibility by (1) showing that AMPAR- and NMDAR-dependent synaptic responses evoked by stimulation of a single spine are reduced by focal co-application of guanfacine and baclofen, (2) showing that α2Rs and $GABA_BRs$ co-localize with PSD95, and (3) finding that guanfacine and baclofen mutually occlude each other's modulation of VGCCs. A second explanation for our data is that one or both of the actions of guanfacine and baclofen occur via distinct, non-cell-autonomous mechanisms. However, we find that loading single cells with a membrane impermeable PKA antagonist occludes the modulation of both AMPARs and NMDARs, arguing that the relevant α2Rs and $GABA_BRs$ are localized to the recorded neuron.

A third possibility is that α2Rs and $GABA_BRs$ are located in the same spines, and the lack of crosstalk is mediated by functional compartmentalization of signaling cascades. This latter

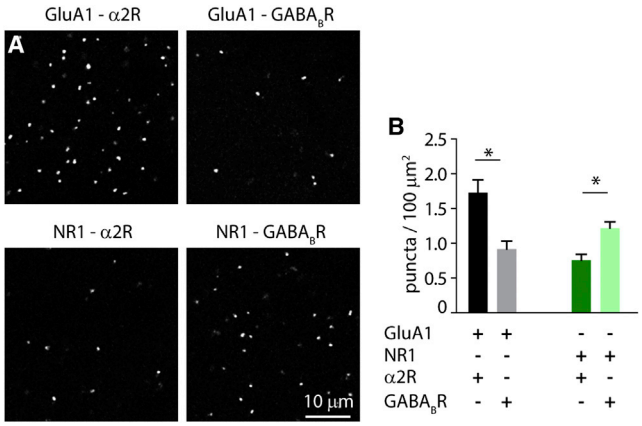

Figure 6. α2Rs Preferentially Localize near AMPARs while GABA$_B$Rs Preferentially Localize near NMDARs

(A) Representative confocal images from PFC sections after proximity ligation assay. Tissue was stained with antibodies against the indicated targets. Bright puncta indicate positive PLA reactions.

(B) Bars indicate mean ± SEM number of puncta per 100 μm^2.

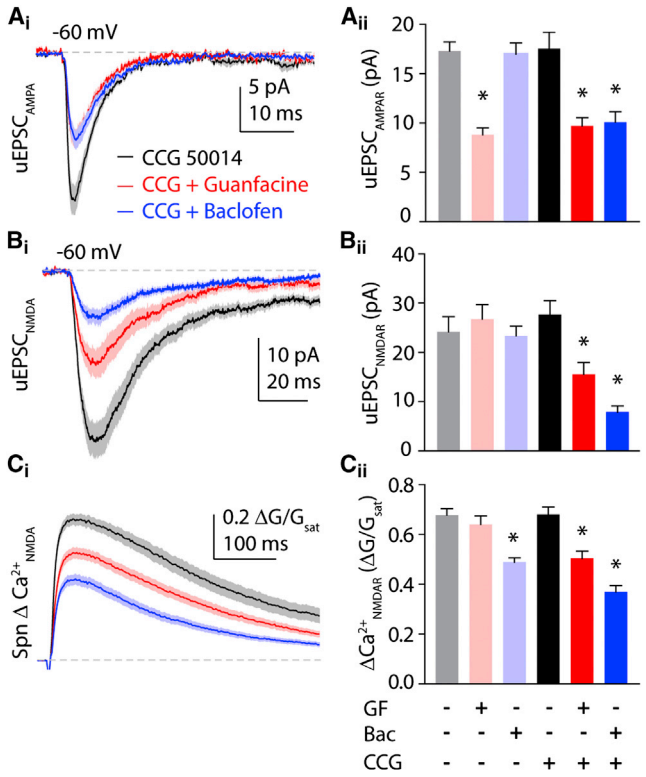

Figure 7. Blocking RGS4 Enables Crosstalk between Modulatory Signaling Pathways

(Ai) AMPAR-mediated currents in the presence of CCG50014 alone (black) or in combination with guanfacine (red) or baclofen (blue).

(Bi and Ci) (Bi) NMDAR-mediated currents and (Ci) Ca^{2+} transients in the presence of the RGS4 inhibitor CCG50014 either alone (black) or in combination with guanfacine (red) or baclofen (blue). Traces show mean ± SEM (solid lines and shaded areas, respectively).

(Aii) Mean amplitude ±SEM of AMPAR-mediated currents in control (gray), guanfacine (pink), and baclofen (light blue), reproduced from Figure 1, or in CCG50014 (black), CCG50014 with guanfacine (red), and CCG50014 with baclofen (blue).

(Bii and Cii) Bars represent mean amplitude ±SEM of NMDAR-mediated currents (Bii) and Ca^{2+} transients (Cii) in control (gray), guanfacine (pink), and baclofen (light blue) from Figure 1, or in CCG50014 (black), CCG50014 with guanfacine (red), and CCG50014 with baclofen (blue).

*$p < 0.05$, Tukey's multiple comparison test.

conclusion is strongly supported by our results, which suggest a novel functional microdomain established by the limited lifetime of $G\alpha_i$, whose signaling is terminated by its endogenous GTPase activity (Arshavsky and Pugh, 1998). The ability of $G\alpha_i$ subunits to hydrolyze GTP is strongly accelerated by Regulators of G protein Signaling (RGS) proteins (Watson et al., 1996). Of this protein family, RGS4 is strongly expressed in layer 5 of the PFC (Ebert et al., 2006). Here, we show that blocking RGS4 activity pharmacologically (CCG50014) or by dialyzing the cells with an antibody against RGS4 impairs the selectivity of $G\alpha_i$-coupled neuromodulators, thus enabling crosstalk of second messenger systems and leading to a breakdown in signal specificity in dendritic spines of layer 5 pyramidal neurons (Figure S8). Notably, previous computational work explicitly predicted a role for RGS4 in restricting $G\alpha_i$ signaling to a small microdomain (Zhong et al., 2003). In this model, high RGS4 activity can limit diffusion of GTP-bound $G\alpha_i$ to <20 nm. This suggestion is supported by our proximity ligation assay data, which suggest preferential postsynaptic coupling of α2Rs/AMPARs and GABA$_B$Rs/NMDARs within 20 nm (Söderberg et al., 2006). There is mounting anatomical evidence that synaptic proteins, including glutamate receptors, are organized into 70- to 80-nm clusters within the postsynaptic density (MacGillavry et al., 2013; Nair et al., 2013). Precedent for such structural links was shown previously for a presynaptic β2-adrenergic-AMPAR signaling complex allowing highly localized cAMP signaling in the hippocampus (Joiner et al., 2010). Here, we demonstrate a functional role for these nano-structures and provide a plausible biochemical mechanism for the segregation of signaling domains within a single synapse.

We note that an additional explanation for our results is that both adrenergic and GABAergic activity stimulates an unidentified non-canonical (e.g., not adenylate cyclase-mediated) signaling pathway that inhibits cross-modulation of glutamate receptors. While possible, this explanation seems unlikely given the findings that two independent methods of blocking RGS4 activity lead to cross-modulation. Thus, this alternative explanation would require the existence of an unidentified GPCR-coupled pathway that is also regulated by RGS4.

Surprisingly, we find that blocking RGS4 activity allows both guanfacine and baclofen to modulate the total current through NMDARs in addition to the Ca^{2+} influx. A similar result was seen when blocking PKA signaling directly with H89. This result suggests a second PKA target on the NMDAR, in addition to GluN2B S1166, such as GluN1 S897, that controls total current magnitude. We propose that modest reduction in PKA signaling (as occurs with activation of GABA$_B$Rs) influences Ca^{2+} influx by selectively dephosphorylating S1166, while stronger reduction in PKA signaling (either with a pharmacological block or the increased activity of $G\alpha_i$ following RGS4 block) leads to

decreased Ca^{2+} and total current by dephosphorylating multiple targets.

Functionally, our findings suggest that distinct modulatory systems coupled to PKA signaling differentially impact synaptic integration. Specifically, adrenergic actions via α2Rs are expected to reduce electrical summation of inputs leading to a reduction in neuronal output. In contrast, GABAergic actions are expected to regulate summation of local dendritic Ca^{2+} signals, potentially influencing synaptic plasticity. Thus, breakdown in the functional segregation of these pathways might lead to aberrant modulation and dysregulation of cellular activity. Indeed, mutations in RGS4 have been linked to neuropsychiatric disorders such as schizophrenia (Levitt et al., 2006). Future studies are necessary to investigate the interactions of RGS4 and neuromodulatory signaling in disease.

EXPERIMENTAL PROCEDURES

Slice Preparation

All animal handling was performed in accordance with guidelines approved by the Yale Institutional Animal Care and Use Committee and federal guidelines. Acute prefrontal cortical (PFC) slices (300 μm) were prepared from wild-type C57/Bl6 mice (P22-36) and maintained in artificial cerebrospinal fluid (ACSF) containing (in mM): 126 NaCl, 26 $NaHCO_3$, 1.25 NaH_2PO_4, 3 KCl, 1 $MgCl_2$, 2 $CaCl_2$, 10 glucose, 0.4 sodium ascorbate, 2 sodium pyruvate, and 3 myo-inositol, bubbled with 95% O_2 and 5% CO_2.

Electrophysiology and Imaging

All experiments were conducted at near physiological temperature (32°C–34°C). For voltage-clamp recordings, glass electrodes (1.8-3.0 MΩ) were filled with internal solution containing (in mM): 135 $CsMeSO_3$, 10 HEPES, 4 $MgCl_2$, 4 Na_2ATP, 0.4 NaGTP, 10 sodium creatine phosphate, and 0.2% Neurobiotin (Vector Laboratories), Alexa Fluor-594 (10 μM), Fluo-5F (300 μM), adjusted to pH 7.3 with CsOH. Electrophysiological recordings were made using a Multiclamp 700B amplifier, filtered at 4 kHz, and digitized at 10 kHz.

Two-photon imaging was accomplished with a custom-modified Olympus BX51-WI microscope. Fluorophores were excited using 840 nm light from a pulsed titanium-sapphire laser and emissions collected by photomultiplier tubes (Hamamatsu).

For focal stimulation of single dendritic spines, we used two-photon laser uncaging of glutamate (2PLU). To photorelease glutamate, a second Ti-Sapphire laser tuned to 720 nm was introduced into the light path using polarization optics. Back propagating action potentials (bAPs) were evoked by injecting brief current pulses (2 nA, 2 ms) into the cell through the recording pipette.

Data Acquisition and Analysis

Imaging and physiology data were acquired using National Instruments data acquisition boards and custom software written in MATLAB. Off-line analysis was performed using custom routines written in MATLAB and IgorPro. Statistical comparisons were conducted in GraphPad Prism 5. Unless otherwise stated, all data were analyzed using two-tailed, unpaired t tests.

Pharmacology and Reagents

2PLU experiments were performed in normal ACSF supplemented with MNI-glutamate (2.5 mM) and D-serine (10 μM). To isolate AMPAR-mediated currents, we added TTX (1 μM), picrotoxin (50 μM), CGP55845 (3 μM), and CPP (10 μM) to the ACSF. To isolate NMDAR-mediated currents, we modified our original ACSF to contain 0 mM Mg and 3 mM Ca^{2+} and included TTX (1 μM), picrotoxin (50 μM), CGP55845 (3 μM), and NBQX 10 μM. In experiments investigating the effects of baclofen, CGP55845 was omitted from the solutions. For PKA pharmacology, we applied H89 (10 μM) or N6-benzo-cAMP (100 μM, Millipore). In some experiments, we included PKI(6-22) (20 μM) in the recording pipette. To block the actions of RGS4, we added CCG50014 (5 μM). All compounds were from Tocris except where noted.

Western Blot Analysis

Brain slices containing the PFC were prepared as described and incubated with normal ACSF for control or ACSF supplemented with either guanfacine 40 μM, baclofen 5 μM, H89 10 μM, or forskolin 50 μM for 10 min at 32°C–34°C before the prefrontal cortex was dissected out, homogenized, and lysed in 20 mM Tris, 1 mM EDTA and 1 × Halt protease and phosphatase inhibitor cocktail and 0.5% SDS (pH 8.0). After centrifugation, samples were separated by SDS-PAGE and transferred to PVDF membranes. Primary antibodies against phosphorylated GluA1 S845, phosphorylated GluN2B S1166 or RGS4 were applied overnight. Bands were visualized using standard HRP procedures. Membranes were then stripped from antibodies, re-blocked, and immunoreacted with non-phospho specific anti-GluA1 or anti-GluN2B primary antibody to establish total amount of GluA1 or GluN2B in the samples. Scanned autoradiography images were analyzed with ImageJ. Phosphorylation was quantified as phoshorylated/total protein and normalized to the control values of each experiment.

Immunofluorescence and Proximity Ligation Assay

C57/bl6 mice were transcardially perfused with phosphate buffer (PB) followed by 4% paraformaldehyde. To expose synaptic proteins, sections (70 μm) containing the PFC were permeabilized with 0.1% Triton X-100 and then treated with 0.25 mg/ml pepsin for 10 min at 37°C in 0.2 N HCl. Primary antibodies against PSD95 or Bassoon, α2R, and $GABA_bR$ were applied overnight. Following secondary antibody staining, images were collected from the PFC region and analyzed in Cell Profiler. Co-localization is given as the percentage of PSD95 or Bassoon puncta overlapping with both α2R and $GABA_BR$ staining.

To perform proximity ligation assay, 70-μm sections containing the PFC were obtained from theee mice and pepsin treated as described. Glutamate receptors were co-labeled with GPCRs using primary antibodies against GluA1 or GluN1 and α2R or $GABA_bR$. Proximity ligation assay (PLA) was performed using a Duolink In Situ kit (Sigma) in accordance with the manufacturer's instructions. Images were randomly collected from the PFC region of the sections and analyzed in Cell Profiler.

SUPPLEMENTAL INFORMATION

Supplemental Information includes Supplemental Experimental Procedures and five figures and can be found with this article online at http://dx.doi.org/10.1016/j.celrep.2015.06.029.

AUTHOR CONTRIBUTIONS

G.L. and M.J.H. designed and performed the experiments, analyzed the data, and wrote the paper.

ACKNOWLEDGMENTS

The authors thank J. Cardin, S. Tomita, and members of M.J.H.'s laboratory for comments during the preparation of this manuscript. The work was funded by grants from the Smith Family Foundation (M.J.H.), The Yale Brown-Coxe Memorial Fund (G.L.), The Brain and Behavior Research Foundation (M.J.H. and G.L.), and the NIH: MH099045 (M.J.H.).

Received: January 8, 2014
Revised: March 14, 2015
Accepted: June 5, 2015
Published: July 2, 2015

REFERENCES

Arnsten, A.F. (2011). Catecholamine influences on dorsolateral prefrontal cortical networks. Biol. Psychiatry *69*, e89–e99.

Arshavsky, V.Y., and Pugh, E.N., Jr. (1998). Lifetime regulation of G protein-effector complex: emerging importance of RGS proteins. Neuron *20*, 11–14.

Blazer, L.L., Zhang, H., Casey, E.M., Husbands, S.M., and Neubig, R.R. (2011). A nanomolar-potency small molecule inhibitor of regulator of G-protein signaling proteins. Biochemistry *50*, 3181–3192.

Carter, A.G., and Sabatini, B.L. (2004). State-dependent calcium signaling in dendritic spines of striatal medium spiny neurons. Neuron *44*, 483–493.

Chalifoux, J.R., and Carter, A.G. (2010). GABAB receptors modulate NMDA receptor calcium signals in dendritic spines. Neuron *66*, 101–113.

Chen, G., Chen, P., Tan, H., Ma, D., Dou, F., Feng, J., and Yan, Z. (2008). Regulation of the NMDA receptor-mediated synaptic response by acetylcholinesterase inhibitors and its impairment in an animal model of Alzheimer's disease. Neurobiol. Aging *29*, 1795–1804.

Destexhe, A., Mainen, Z.F., and Sejnowski, T.J. (1994). Synthesis of models for excitable membranes, synaptic transmission and neuromodulation using a common kinetic formalism. J. Comput. Neurosci. *1*, 195–230.

Dismukes, R.K. (1979). New concepts of molecular communication among neurons. Behav. Brain Sci. *2*, 409–416.

Ebert, P.J., Campbell, D.B., and Levitt, P. (2006). Bacterial artificial chromosome transgenic analysis of dynamic expression patterns of regulator of G-protein signaling 4 during development. I. Cerebral cortex. Neuroscience *142*, 1145–1161.

Esteban, J.A., Shi, S.H., Wilson, C., Nuriya, M., Huganir, R.L., and Malinow, R. (2003). PKA phosphorylation of AMPA receptor subunits controls synaptic trafficking underlying plasticity. Nat. Neurosci. *6*, 136–143.

Gamo, N.J., and Arnsten, A.F. (2011). Molecular modulation of prefrontal cortex: rational development of treatments for psychiatric disorders. Behav. Neurosci. *125*, 282–296.

Gold, S.J., Ni, Y.G., Dohlman, H.G., and Nestler, E.J. (1997). Regulators of G-protein signaling (RGS) proteins: region-specific expression of nine subtypes in rat brain. J. Neurosci. *17*, 8024–8037.

Herlitze, S., Garcia, D.E., Mackie, K., Hille, B., Scheuer, T., and Catterall, W.A. (1996). Modulation of Ca2+ channels by G-protein beta gamma subunits. Nature *380*, 258–262.

Higley, M.J., and Sabatini, B.L. (2008). Calcium signaling in dendrites and spines: practical and functional considerations. Neuron *59*, 902–913.

Ji, X.H., Ji, J.Z., Zhang, H., and Li, B.M. (2008). Stimulation of alpha2-adrenoceptors suppresses excitatory synaptic transmission in the medial prefrontal cortex of rat. Neuropsychopharmacology *33*, 2263–2271.

Joiner, M.L., Lisé, M.F., Yuen, E.Y., Kam, A.Y., Zhang, M., Hall, D.D., Malik, Z.A., Qian, H., Chen, Y., Ulrich, J.D., et al. (2010). Assembly of a beta2-adrenergic receptor—GluR1 signalling complex for localized cAMP signalling. EMBO J. *29*, 482–495.

Kesner, R.P., and Churchwell, J.C. (2011). An analysis of rat prefrontal cortex in mediating executive function. Neurobiol. Learn. Mem. *96*, 417–431.

Knight, A.R., and Bowery, N.G. (1996). The pharmacology of adenylyl cyclase modulation by GABAB receptors in rat brain slices. Neuropharmacology *35*, 703–712.

Kulik, A., Vida, I., Lujan, R., Haas, C.A., Lopez-Bendito, G., Shigemoto, R., and Frotscher, M. (2003). Subcellular localization of metabotropic GABA(B) receptor subunits GABA(B1a/b) and GABA(B2) in the rat hippocampus. J. Neurosci. *23*, 11026–11035.

Levitt, P., Ebert, P., Mirnics, K., Nimgaonkar, V.L., and Lewis, D.A. (2006). Making the case for a candidate vulnerability gene in schizophrenia: convergent evidence for regulator of G-protein signaling 4 (RGS4). Biol. Psychiatry *60*, 534–537.

Lisman, J.E., Raghavachari, S., and Tsien, R.W. (2007). The sequence of events that underlie quantal transmission at central glutamatergic synapses. Nat. Rev. Neurosci. *8*, 597–609.

Liu, W., Yuen, E.Y., Allen, P.B., Feng, J., Greengard, P., and Yan, Z. (2006). Adrenergic modulation of NMDA receptors in prefrontal cortex is differentially regulated by RGS proteins and spinophilin. Proc. Natl. Acad. Sci. USA *103*, 18338–18343.

MacGillavry, H.D., Song, Y., Raghavachari, S., and Blanpied, T.A. (2013). Nanoscale scaffolding domains within the postsynaptic density concentrate synaptic AMPA receptors. Neuron *78*, 615–622.

Murphy, J.A., Stein, I.S., Lau, C.G., Peixoto, R.T., Aman, T.K., Kaneko, N., Aromolaran, K., Saulnier, J.L., Popescu, G.K., Sabatini, B.L., et al. (2014). Phosphorylation of Ser1166 on GluN2B by PKA is critical to synaptic NMDA receptor function and Ca2+ signaling in spines. J. Neurosci. *34*, 869–879.

Nair, D., Hosy, E., Petersen, J.D., Constals, A., Giannone, G., Choquet, D., and Sibarita, J.B. (2013). Super-resolution imaging reveals that AMPA receptors inside synapses are dynamically organized in nanodomains regulated by PSD95. J. Neurosci. *33*, 13204–13224.

Raymond, L.A., Tingley, W.G., Blackstone, C.D., Roche, K.W., and Huganir, R.L. (1994). Glutamate receptor modulation by protein phosphorylation. J. Physiol. Paris *88*, 181–192.

Sabatini, B.L., and Svoboda, K. (2000). Analysis of calcium channels in single spines using optical fluctuation analysis. Nature *408*, 589–593.

Söderberg, O., Gullberg, M., Jarvius, M., Ridderstråle, K., Leuchowius, K.J., Jarvius, J., Wester, K., Hydbring, P., Bahram, F., Larsson, L.G., and Landegren, U. (2006). Direct observation of individual endogenous protein complexes in situ by proximity ligation. Nat. Methods *3*, 995–1000.

Stan, A.D., and Lewis, D.A. (2012). Altered cortical GABA neurotransmission in schizophrenia: insights into novel therapeutic strategies. Curr. Pharm. Biotechnol. *13*, 1557–1562.

Summers, R.J., and McMartin, L.R. (1993). Adrenoceptors and their second messenger systems. J. Neurochem. *60*, 10–23.

Turner, E.M., Blazer, L.L., Neubig, R.R., and Husbands, S.M. (2012). Small molecule inhibitors of regulator of g protein signalling (RGS) proteins. ACS Med. Chem. Lett. *3*, 146–150.

Tyacke, R.J., Lingford-Hughes, A., Reed, L.J., and Nutt, D.J. (2010). GABAB receptors in addiction and its treatment. Adv. Pharmacol. *58*, 373–396.

Wang, M., Ramos, B.P., Paspalas, C.D., Shu, Y., Simen, A., Duque, A., Vijayraghavan, S., Brennan, A., Dudley, A., Nou, E., et al. (2007). Alpha2A-adrenoceptors strengthen working memory networks by inhibiting cAMP-HCN channel signaling in prefrontal cortex. Cell *129*, 397–410.

Watson, N., Linder, M.E., Druey, K.M., Kehrl, J.H., and Blumer, K.J. (1996). RGS family members: GTPase-activating proteins for heterotrimeric G-protein alpha-subunits. Nature *383*, 172–175.

Yan, Z., and Surmeier, D.J. (1996). Muscarinic (m2/m4) receptors reduce N- and P-type Ca2+ currents in rat neostriatal cholinergic interneurons through a fast, membrane-delimited, G-protein pathway. J. Neurosci. *16*, 2592–2604.

Yuste, R., Majewska, A., and Holthoff, K. (2000). From form to function: calcium compartmentalization in dendritic spines. Nat. Neurosci. *3*, 653–659.

Zhong, H., Wade, S.M., Woolf, P.J., Linderman, J.J., Traynor, J.R., and Neubig, R.R. (2003). A spatial focusing model for G protein signals. Regulator of G protein signaling (RGS) protien-mediated kinetic scaffolding. J. Biol. Chem. *278*, 7278–7284.

Cell Reports
Supplemental Information

Glutamate Receptor Modulation Is Restricted to Synaptic Microdomains

Gyorgy Lur and Michael J. Higley

Supplemental Figures

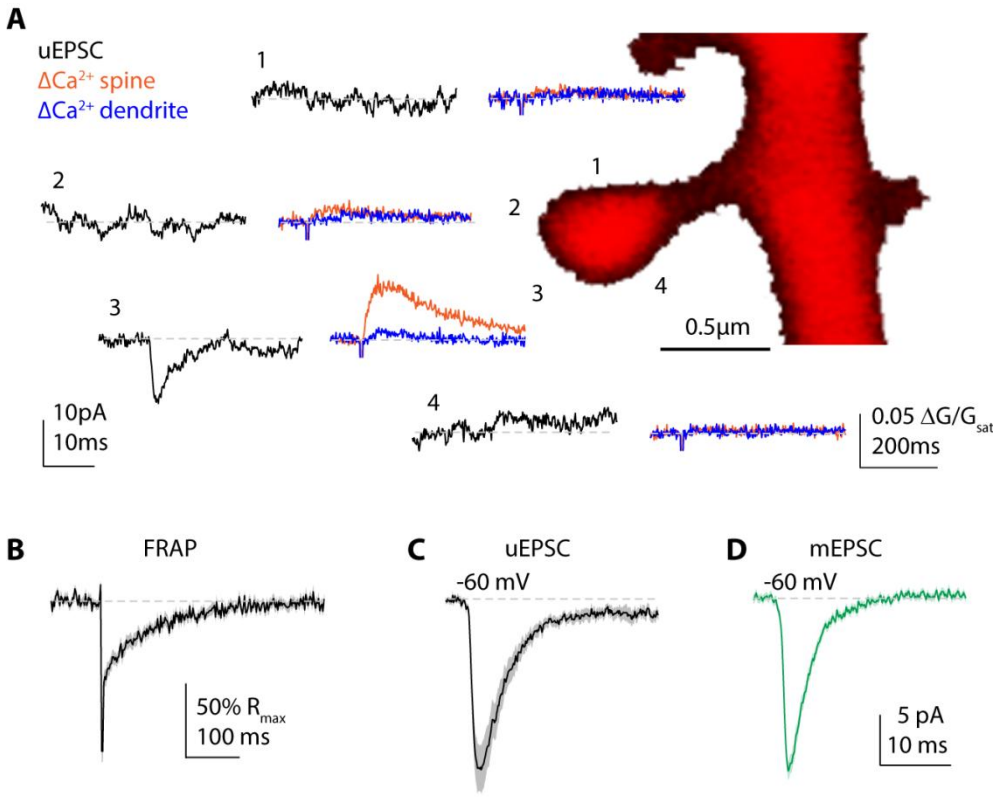

Figure S1. Calibration of 2PLU at a single dendritic spine. (**A**) Probing multiple uncaging sites (numbers) around a single spine head. Black traces show somatic excitatory post synaptic currents (uEPSCs) while colored traces represent Ca^{2+} transients in the spine head (red) and the neighboring dendritic shaft (blue) evoked at the positions indicated by their respective numbers. (**B**) The power output of the uncaging Ti-Sapphire laser is adjusted so that, when positioned over the spine head, it produces 50% photobleaching of the Alexa594 dye that rapidly recovers after the stimulus (fluorescent recovery after photobleaching – FRAP). (**C**) The size and kinetics of uEPSCs evoked by 2PLU at the established 50% FRAP laser power (n=18 spines) are comparable to (**D**) miniature EPSCs (n=161 events) measured in the same cells (n=4 cells). Traces show mean ± SEM (solid line and shaded area, respectively).

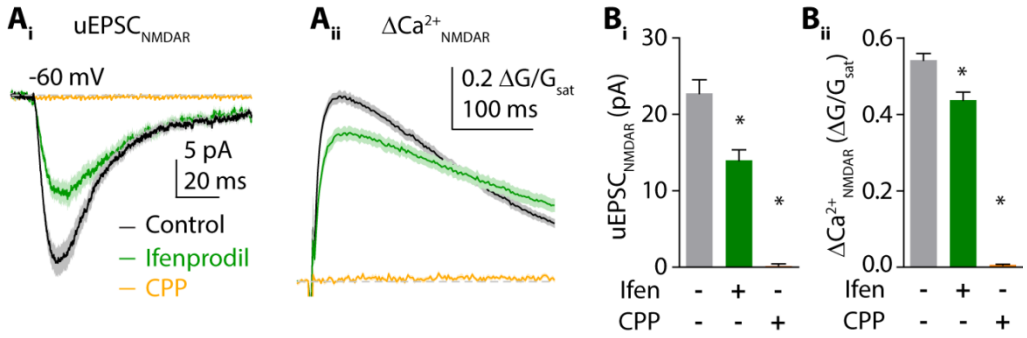

Figure S2. Characteristics of NMDAR-mediated currents and Ca^{2+} transients. (**Ai**) Mean ± SEM traces (solid lines and shaded areas) of 2PLU-evoked NMDAR-mediated uEPSCs and (**Aii**) Ca^{2+} transients from single spines in control (black, n=46 spines), ifenprodil (green, n=33 spines), and CPP (orange, n=12 spines). (**Bi**) Bar graphs represent mean ± SEM amplitude of uEPSCs and (**Bii**) Ca^{2+} transients in control (gray) versus ifenprodil (green) or CPP (orange). *: $p<0.05$, two tailed, unpaired t-test.

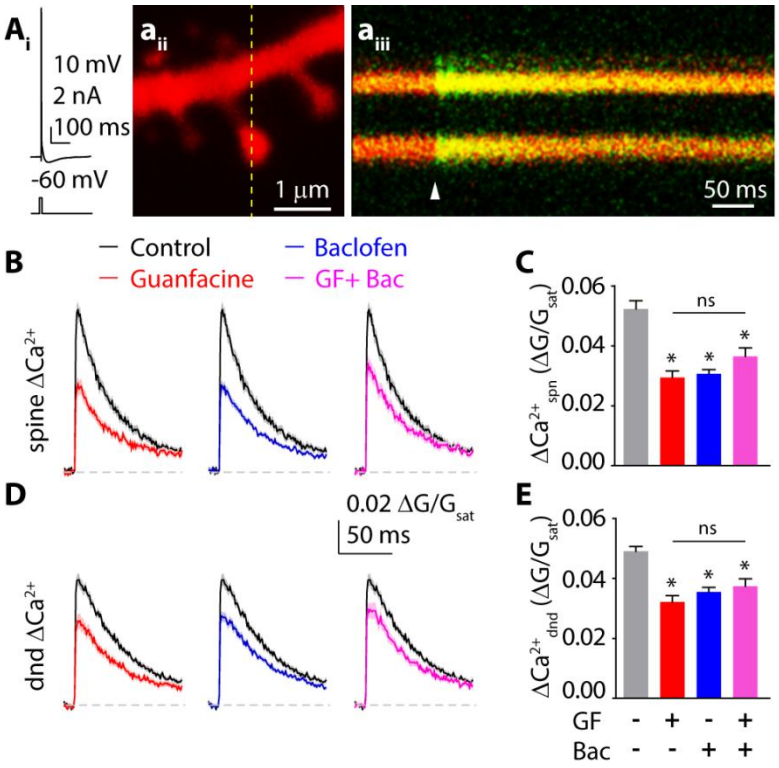

Figure S3. α2Rs and $GABA_B$Rs modulate Ca^{2+} transients evoked by back-propagating action potentials. (**Ai**) Example action potential (top) evoked by somatic current injection (bottom). (**Aii**) 2-photon image of a dendritic spine and (**Aiii**) fluorescence trace acquired in the line scan indicated by dashed line in (**Aii**). White arrowhead indicates the timing of the AP. (**B**) Mean ± SEM (solid lines and shaded areas, respectively) traces of bAP-evoked Ca^{2+} transients in control (black), guanfacine (red), baclofen (blue), or guanfacine combined with baclofen (magenta) in the spine head. (**C**) Bar graphs show the mean Ca^{2+} transient amplitude ± SEM. (**D**-**E**) Same as (**B**-**C**) for Ca^{2+} transients in the dendritic shaft. *: $p<0.05$, Tukey`s multiple comparison test.

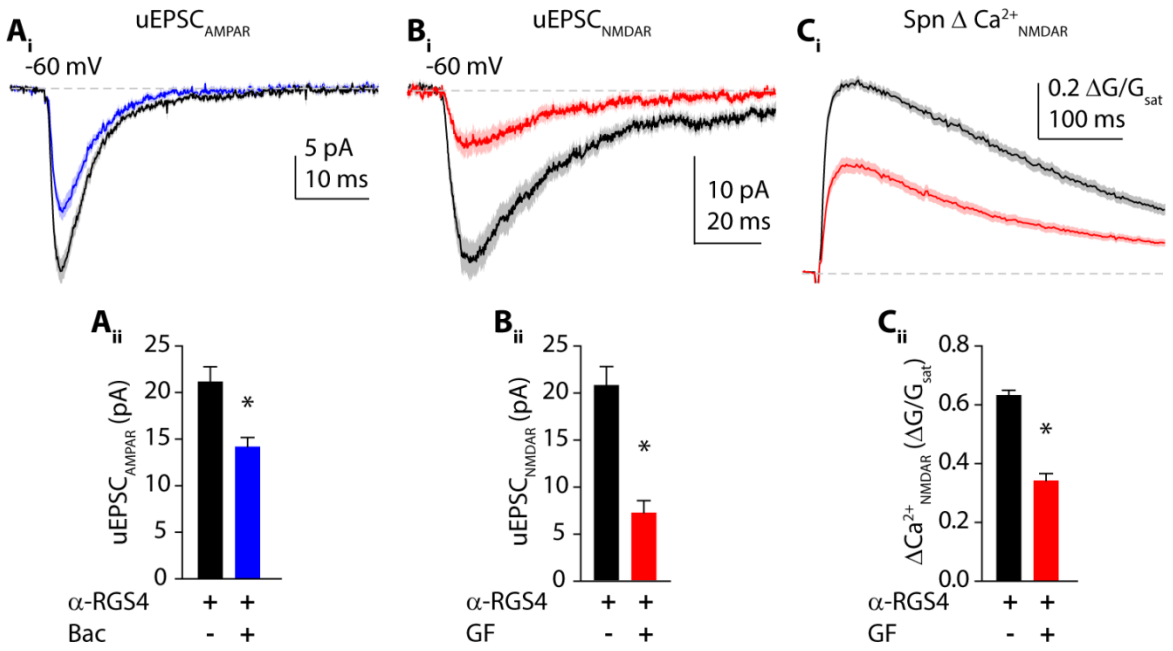

Figure S4. Dialysis with anti-RGS4 antibody enables cross-talk between α2R and $GABA_BR$ signaling. The internal solution contains an antibody specifically binding RGS4. (**Ai**) Mean (solid lines) ± SEM traces (shaded areas) of AMPAR-mediated currents in control (n=31 spines, black) and in baclofen (n=34 spines, blue). (**Bi**) Mean ± SEM traces (solid lines and shaded areas, respectively) of 2PLU-evoked, NMDAR-mediated uEPSCs and (**Ci**) Ca^{2+} transients in control (n=30 spines, black) and in guanfacine (n=32 spines, red). (**Aii**) Bars show mean ± SEM of AMPAR currents in control (black and baclofen (blue). (**Bii**) Bars represent mean ± SEM of NMDAR-mediated currents and (**Cii**) ΔCa^{2+} in control (black) and in guanfacine (red). *: $p<0.05$, unpaired t-test.

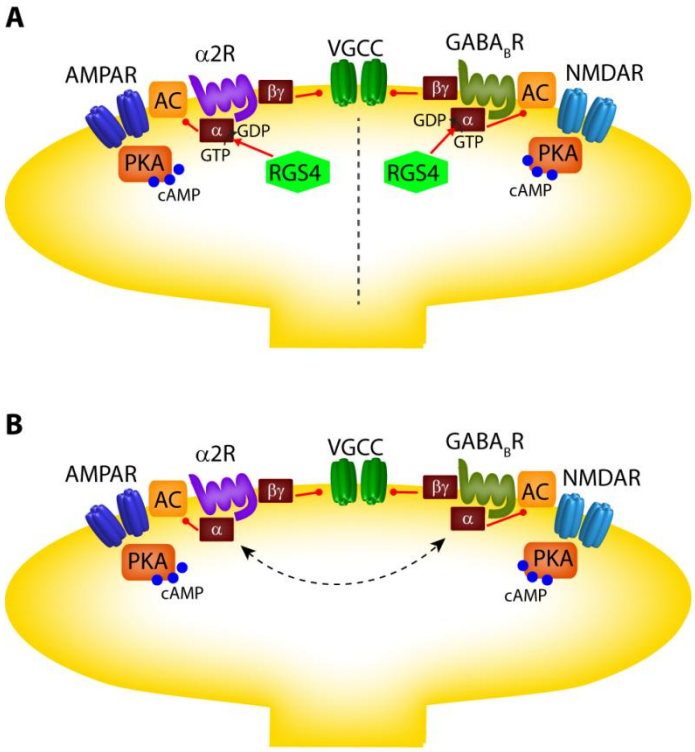

Figure S5. RGS4 restricts Gα_i mobility promoting segregated PKA-dependent regulation of glutamate receptors. Schematic shows α2R and GABA$_B$R signaling pathways targeting AMPARs and NMDARs, respectively. Both cascades utilize Gα_i subunits to block cAMP production by inhibiting adenylate cyclase (AC) activity. This in turn reduces PKA-dependent phosphorylation of the target glutamate receptor. VGCCs are modulated by the membrane delimited G$\beta\gamma$ subunits in a PKA-independent manner. (**A**) Cross-talk between modulatory pathways targeting AMPARs and NMDARs is restricted by RGS4 activity promoting signaling microdomains within the spine head. (**B**) Blocking RGS4 removes the selectivity of α2Rs and GABA$_B$Rs towards their respective glutamate receptors.

Supplemental Experimental procedures:

Slice Preparation

All animal handling was performed in accordance with guidelines approved by the Yale Institutional Animal Care and Use Committee and federal guidelines. Glutamate uncaging experiments were conducted using acute prefrontal cortical (PFC) slices from wild-type C57/Bl6 mice (P22-36). Under isoflurane anesthesia, mice were decapitated and coronal slices (300 µm) were cut in ice-cold external solution containing (in mM): 110 choline, 25 $NaHCO_3$, 1.25 NaH_2PO_4, 3 KCl, 7 $MgCl_2$, 0.5 $CaCl_2$, 10 glucose, 11.6 sodium ascorbate and 3.1 sodium pyruvate, bubbled with 95% O_2 and 5% CO_2. Slices containing the prelimbic-infralimbic regions of the PFC were then transferred to artificial cerebrospinal fluid (ACSF) containing (in mM): 126 NaCl, 26 $NaHCO_3$, 1.25 NaH_2PO_4, 3 KCl, 1 $MgCl_2$, 2 $CaCl_2$, 10 glucose, 0.4 sodium ascorbate, 2 sodium pyruvate and 3 myo-inositol, bubbled with 95% O_2 and 5% CO_2. After an incubation period of 15 min at 34 °C, the slices were maintained at 22–24 °C for at least 20 min before use.

Electrophysiology and imaging

All experiments were conducted at near physiological temperature (32-34°C) in a submersion-type recording chamber. Whole-cell patch-clamp recordings were obtained from layer 5 pyramidal cells (400-500 µm from the pial surface) identified with video-infrared/differential interference contrast. For voltage-clamp recordings, glass electrodes (1.8-3.0 MΩ) were filled with internal solution containing (in mM): 135 $CsMeSO_3$, 10 HEPES, 4 $MgCl_2$, 4 Na_2ATP, 0.4 NaGTP, 10 sodium creatine phosphate and 0.2% Neurobiotin (Vector Laboratories) adjusted to pH 7.3 with CsOH. For current-clamp recordings (Fig. S3, potassium was substituted for cesium. Red-fluorescent Alexa Fluor-594 (10 µM, Invitrogen) and the green-fluorescent calcium (Ca^{2+})-sensitive Fluo-5F (300 µM, Invitrogen) were included in the pipette solution to visualize cell morphology and changes of intracellular Ca^{2+} concentration, respectively. Neurons were filled via the patch electrode for 10 min before imaging. In experiments for Fig. S4, we added an RGS4 antibody (Millipore, RBT17) at 1:100 dilution to the internal solution and substituted Cs-gluconate for $CsMeSO_3$ to improve giga-seal formation. Cells were dialyzed with the anti-RGS4 antibody for 10 minutes before imaging. For whole-cell voltage-clamp recordings, series resistance was 10-22 MΩ and uncompensated. Electrophysiological recordings were made using a Multiclamp 700B amplifier (Molecular Devices), filtered at 4 kHz, and digitized at 10 kHz.

2-photon imaging was accomplished with a custom-modified Olympus BX51-WI microscope (Olympus, Japan), including components manufactured by Mike's Machine Company (Higley and Sabatini, 2010). Fluorophores were excited using 840 nm light from a pulsed titanium-sapphire laser (Ultra2, Coherent). Emitted green and red photons were separated with appropriate optics (Chroma, Semrock) and collected by photomultiplier tubes (Hamamatsu).

For Ca^{2+} imaging, signals were collected during 500 Hz line scans across a spine and the neighboring dendritic shaft. Reference frame scans were taken between each acquisition to correct for small spatial drift over time. Ca^{2+} signals were first quantified as increases in green fluorescence from baseline normalized to the average red fluorescence ($\Delta G/R$). We then expressed fluorescence changes as the fraction of the G/R ratio measured in saturating Ca^{2+} ($\Delta G/G_{sat}$). To calculate G_{sat}, we imaged a 1:1 mixture of internal solution and 1 M $CaCl_2$ in a sealed recording pipette in the specimen plane under conditions identical to those used during recordings. Normalizing G/R to the saturated Ca^{2+} signal compensates for variations in fluorophore concentration and optical collection efficiency across experiments and laboratories.

2-Photon Glutamate uncaging and bAP activation

For focal stimulation of single dendritic spines, we used 2-photon laser uncaging of glutamate (2PLU). To photorelease glutamate, a second Ti-Sapphire laser tuned to 720 nm was introduced into the light path using polarization optics. Laser power was calibrated for each spine by directing the uncaging spot to the middle of the spine head. We adjusted uncaging power to achieve 50% photobleaching of the Alexa 594 dye filling the spine (Fig. S1). The power used for 2PLU ranged from 8 to 25 mW. For synaptic stimulation, we typically uncaged glutamate at 3-4 separate locations around a single spine head to find a "hot spot", the place of the largest response (Fig. S1). Back propagating action potentials (bAPs) were evoked by injecting brief current pulses (2 nA, 2 ms) into the cell through the recording pipette.

Data acquisition and analysis

Imaging and physiology data were acquired using National Instruments data acquisition boards and custom software written in MATLAB (Mathworks, (Pologruto et al., 2003)). Off-line analysis was performed using custom routines written in MATLAB and IgorPro (Wavemetrics). AMPAR-mediated EPSC amplitudes were calculated by finding the peak of the current traces and averaging the values within a 0.3 ms window. NMDAR-mediated currents were measured in a 3 ms window around the peak for isolated responses and 140 ms after the stimulus for non-isolated responses collected at +40 mV. 2PLU or AP-evoked ΔCa^{2+} was calculated as the average $\Delta G/G_{sat}$ over a 100 ms window, starting 5 ms after the uncaging or the AP was triggered. Statistical comparisons were conducted in GraphPad Prism 5. Unless otherwise stated, all data were analyzed using two-tailed, unpaired T-tests.

Pharmacology and reagents

2PLU experiments were performed in normal ACSF supplemented with MNI-glutamate (2.5 mM) and D-serine (10 μM). To isolate AMPAR-mediated currents in voltage clamp experiments, we added TTX (1 μM), picrotoxin (50 μM), CGP55845 (3 μM), and CPP (10 μM) to the ACSF. To isolate NMDAR-mediated currents, we modified our original ACSF to contain 0 mM Mg and 3 mM Ca^{2+} and included TTX (1 μM), picrotoxin (50 μM), CGP55845 (3 μM), and NBQX 10 μM. To selectively block GluN2B containing NMDARs in some experiments we included ifenprodil (3 μM) in the ACSF. In experiments investigating the effects of baclofen, CGP55845 was omitted from the solutions. For PKA pharmacology, we applied H89 (10 μM) or N6-benzo-cAMP (100 μM, Millipore). In some experiments, we included PKI(6-22) (20 μM) in the recording pipette. To block the actions of RGS4 we added CCG50014 (5 μM). All compounds were from Tocris except where noted.

Western blot analysis

For RGS4, phospho-GluA1 (S845) and phospho-GluN2B (S1166) western blot analysis, we prepared 300 μm thick brain slices containing the PFC from p22-42 C57/bl6 mice as described above. Following the recovery period, slices were distributed between 5 holding chambers containing normal ACSF for control or ACSF supplemented with either guanfacine 40 μM, baclofen 5 μM, H89 10 μM or forskolin 50 μM. Holding chambers were then incubated for an additional 10 minutes at 32-34°C before the prefrontal cortex was dissected out of the slices on ice. Tissue samples were homogenized and sonicated in ice cold lysis buffer containing 20 mM Tris, 1 mM EDTA and 1x Halt protease and phosphatase inhibitor cocktail (Thermo Scientific) and 0.5% SDS, pH 8.0. After a 10 minute centrifugation at 14000 rpm, the supernatant was collected and protein content was determined using Pierce BCA Protein Assay (Thermo Scientific). Samples containing equal amounts of protein were separated on a 6% poly-acrylamide gel and transferred to PVDF membranes. After blocking for 1h at room temperature with 3% non-fat milk and 0.02% Na-azide in Tris buffered salt solution with 0.05% Tween 20 (TBST), membranes were immunoreacted with primary antibody against phosphorylated

GluA1 S845 (Millipore, 04-1073), phosphorylated GluN2B S1166 (a generous gift from Suzanne Zukin, Albert Einstein College of Medicine) or RGS4 (Millipore, RBT17) in 1% milk and 0.02% Na-azide in TBST, 1:1000, overnight. After washing off excess primary antibody and incubation with the appropriate HRP conjugated secondary antibody (GE Healthcare, UK) for 2 hours at room temperature in TBST, bands were visualized using HyGlo Chemiluminescent HRP Antibody Detection Reagent (Denville Scientific Inc.) and exposed onto autoradiography film (Denville Scientific Inc.). Membranes were then stripped from antibodies using Restore Plus Western Blot Stripping Buffer (15 minutes at room temperature, Thermo Scientific), re-blocked and immunoreacted with non-phospho specific anti-GluA1 (generously provided by Susumu Tomita, Yale University) or anti-GluN2B (Millipore, MAB5778) primary antibody followed by the appropriate HRP-secondary antibody to establish total amount of GluA1 or GluN2B in the samples. Autoradiography films were developed in a Kodak automatic developer, then scanned and analyzed with ImageJ. Phosphorylation was quantified as phoshorylated / total protein and normalized to the control values of each experiment.

Immunofluorescence and proximity ligation assay (PLA)

C57/bl6 mice (p22-40) were transcardially perfused with ice cold phosphate buffer (PB) followed by ice cold 4% paraformaldehyde (PFA, Electron Microscopy Sciences) in PB. After dissection, brains were post-fixed in 4% PFA for 3.5 hours at 4 °C. Sections (70 μm) containing the prefrontal cortex were cut on a vibrotome (Leica) and washed in PB. To expose synaptic proteins tissue sections were permeabilised with 0.1% Triton X-100 (SIGMA) in PB then treated with 0.25 mg/ml pepsin for 10 minutes at 37 °C in 0.2 N HCl. Nonspecific antibody binding was blocked in 10% normal goat serum (NGS, SIGMA) and 1% bovine serum albumin (BSA, SIGMA) in PB for 1 hour. To co-label GPCRs with the postsynaptic marker PSD95 or the presynaptic marker Bassoon, primary antibodies against PSD95 (UC Davis/NIH NeuroMab Facility, 75-028, 1:400 dilution) or Bassoon (Synaptic Systems, 141-021, 1:200), α2R (Neuromics, RA14110, 1:400) and $GABA_bR$ (Millipore, AB2255, 1:400) in 5% NGS, 1% BSA, 0.1% Triton X-100, 0.02% NaN3 in PB were applied overnight at 4 °C. Appropriate secondary antibodies labelled with Alexa 488 (1:1000), Alexa 555 (1:500) and Alexa 647 (1:500) (Invitrogen) were applied for 2 hours. Then sections were mounted on glass microscope slides with ProlongGold (Invitrogen). Images were randomly collected from the prefrontal cortical region of the sections (up to 20 images per mouse for both PSD95 and Bassoon, 4 mice total) using a Leica SP2 inverted confocal microscope (Leica Microsystems) with a 63x oil immersion objective at 10x optical zoom with the pinhole set to 1 Airy unit. Images were then analysed in Cell Profiler (Broad Institute) utilizing object detection to calculate the co-localization of GPCRs with pre- and postsynaptic markers. Images were then shifted by 15 pixels diagonally in ImageJ and re-analyzed with the same pipeline in Cell Profiler. Co-localization is given as the percentage of PSD95 or Bassoon puncta overlapping with both α2R and $GABA_BR$ staining.

To perform proximity ligation assay (PLA), 70 μm sections containing the prefrontal cortex were obtained from 3 mice and pepsin treated as described above. After blocking non-specific antibody binding with 10% donkey serum and 1% BSA in PB for 1 hour, glutamate receptors were co-labelled with GPCRs using primary antibodies against GluA1 (Synaptic Systems, 182 011, 1:2000) or GluN1 (BD Biosciences, 556308, 1:1000) and α2R (Neuromics RA14110, 1:2000) or $GABA_bR$ (Alomone Labs, AGB-001, 1:2000) overnight at 4 °C. Tissue sections were then mounted on microscope slides and PLA was performed using a Duolink In Situ kit (SIGMA) in accordance with the manufacturer's instructions. Briefly, primary antibodies were washed off in wash buffer A (Tris buffered saline with Tween 20, pH 7.4) and sections were incubated with PLA probes, diluted 1:5 in the supplied antibody diluent at 37 °C for 2 hours. PLA probes were then washed off with buffer A and sections were incubated with the Ligase, diluted 1:40 in Ligation buffer, for 1 hour at 37 °C. The tissue was then washed in buffer A and the signal was amplified for 30 minutes at 37 °C using the Polymerase diluted 1:80 in Amplification buffer. Sections were then washed in buffer B (Tris buffer saline, pH 7.5) and a coverslip was mounted

on the slide with Duolink In Situ Mounting Medium. Images were randomly collected from the prefrontal cortical region of the sections (10-11 images for each antibody pair from each mouse) on a Leica SP2 confocal microscope with a 63x oil immersion objective at 3x optical zoom with the pinhole set to 1 Airy unit. Fluorescent puncta were counted using object recognition in Cell Profiler.

Supplemental References

Higley, M.J., and Sabatini, B.L. (2010). Competitive regulation of synaptic Ca2+ influx by D2 dopamine and A2A adenosine receptors. Nature neuroscience *13*, 958-966.

Pologruto, T.A., Sabatini, B.L., and Svoboda, K. (2003). ScanImage: flexible software for operating laser scanning microscopes. Biomedical engineering online *2*, 13.